

LETTER

Simulating twistronics in acoustic metamaterials

To cite this article: S Minhal Gardezi *et al* 2021 *2D Mater.* **8** 031002

View the [article online](#) for updates and enhancements.

You may also like

- [Electronic localization in small-angle twisted bilayer graphene](#)
V Hung Nguyen, D Paszko, M Lamparski et al.
- [Moiré engineering of spin-orbit coupling in twisted platinum diselenide](#)
Lennart Klebl, Qiaoling Xu, Ammon Fischer et al.
- [Incommensurability-induced sub-ballistic narrow-band-states in twisted bilayer graphene](#)
Miguel Gonçalves, Hadi Z Olyaei, Bruno Amorim et al.

2D Materials



LETTER

Simulating twistronics in acoustic metamaterials

RECEIVED
7 December 2020

REVISED
15 March 2021

ACCEPTED FOR PUBLICATION
26 March 2021

PUBLISHED
13 April 2021

S Minhal Gardezi¹ , Harris Pirie² , Stephen Carr³ , William Dorrell² and Jennifer E Hoffman^{1,2,*}

¹ School of Engineering and Applied Sciences, Harvard University, Cambridge, MA 02138, United States of America

² Department of Physics, Harvard University, Cambridge, MA 02138, United States of America

³ Brown Theoretical Physics Center and Department of Physics, Brown University, Providence, RI 02912-1843, United States of America

* Author to whom any correspondence should be addressed.

E-mail: jhoffman@physics.harvard.edu

Keywords: twistronics, twisted bilayer graphene, acoustic metamaterial

Supplementary material for this article is available [online](#)

Abstract

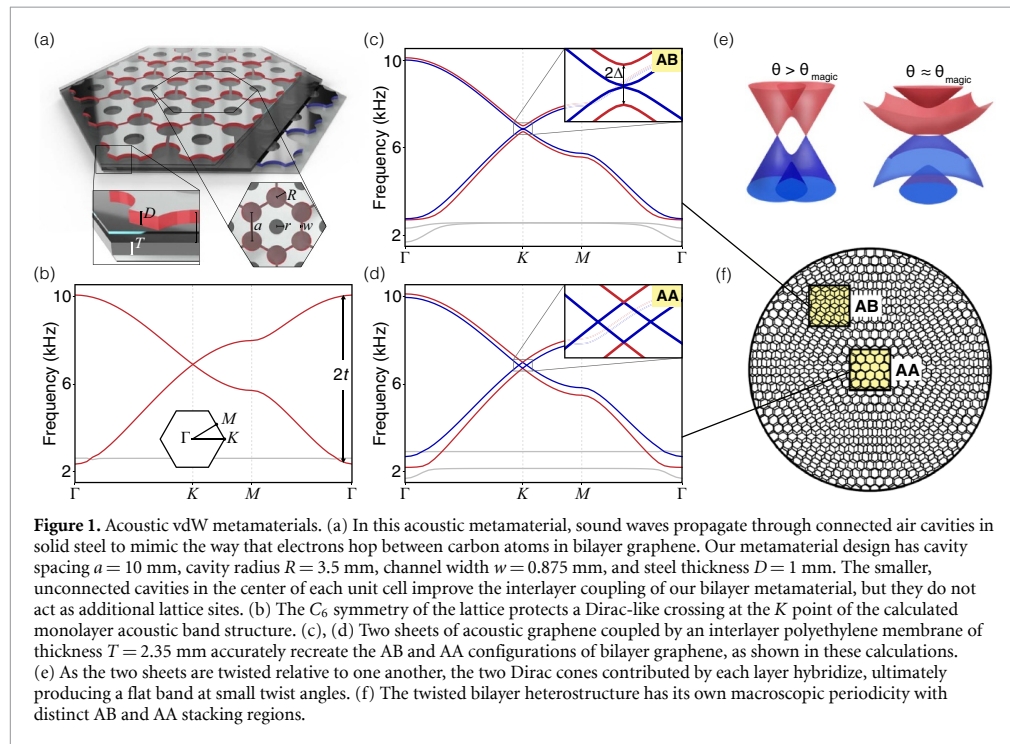
Twisted van der Waals heterostructures have recently emerged as a tunable platform for studying correlated electrons. However, these materials require laborious and expensive effort for both theoretical and experimental exploration. Here we numerically simulate twistronic behavior in acoustic metamaterials composed of interconnected air cavities in two stacked steel plates. Our classical analog of twisted bilayer graphene perfectly replicates the band structures of its quantum counterpart, including mode localization at a magic angle of 1.12° . By tuning the thickness of the interlayer membrane, we reach a regime of strong interlayer tunneling where the acoustic magic angle appears as high as 6.01° , equivalent to applying 130 GPa to twisted bilayer graphene. In this regime, the localized modes are over five times closer together than at 1.12° , increasing the strength of any emergent non-linear acoustic couplings.

1. Introduction

Van der Waals (vdW) heterostructures host a diverse set of useful emergent properties that can be customized by varying the stacking configuration of sheets of two-dimensional (2D) materials, such as graphene, other xenes, or transition-metal dichalcogenides [1–4]. Recently, the possibility of including a small twist angle between adjacent layers in a vdW heterostructure has led to the growing field of twistronics [5]. The twist angle induces a moiré pattern that acts as a tunable potential for electrons moving within the layers, promoting enhanced electron correlations when their kinetic energy is reduced below their Coulomb interaction. Even traditional non-interacting materials can reach this regime, as exemplified by the correlated insulating state in twisted bilayer graphene [6]. Already, vdW heterostructures with moiré superlattices have led to new platforms for Wigner crystals [7], interlayer excitons [8–10], and unconventional superconductivity [11–13]. But the search for novel twistronic phases is still in its infancy and there are countless vdW stacking and twisting arrangements that remain unexplored. Theoretical investigations of these new arrangements are limited

by the large and complex moiré patterns created by multiple small twist angles. Meanwhile, fabrication of vdW heterostructures is restricted to the symmetries and properties of the few freestanding monolayers available today. It remains pressing to develop a more accessible platform to rapidly prototype and explore new twistronic materials to accelerate their technological advancement.

The development of acoustic metamaterials over the last few years has unlocked a compelling platform to guide the design of new quantum materials [14]. Whereas quantum materials can be difficult to predict and fabricate, acoustic metamaterials have straightforward governing equations, continuously tunable properties, fast build times, and inexpensive characterization tools, making them attractive testbeds to rapidly explore their quantum counterparts. Sound waves in an acoustic metamaterial can be reshaped to mimic the collective motion of electrons in a crystalline solid. These acoustic devices can recreate many phenomena seen in quantum materials, such as chiral Landau levels [15], higher-order topology [16, 17], and fragile topology [18]. In vdW systems, the Dirac-like electronic bands in graphene have been mimicked using longitudinal acoustics [19–21], surface acoustic



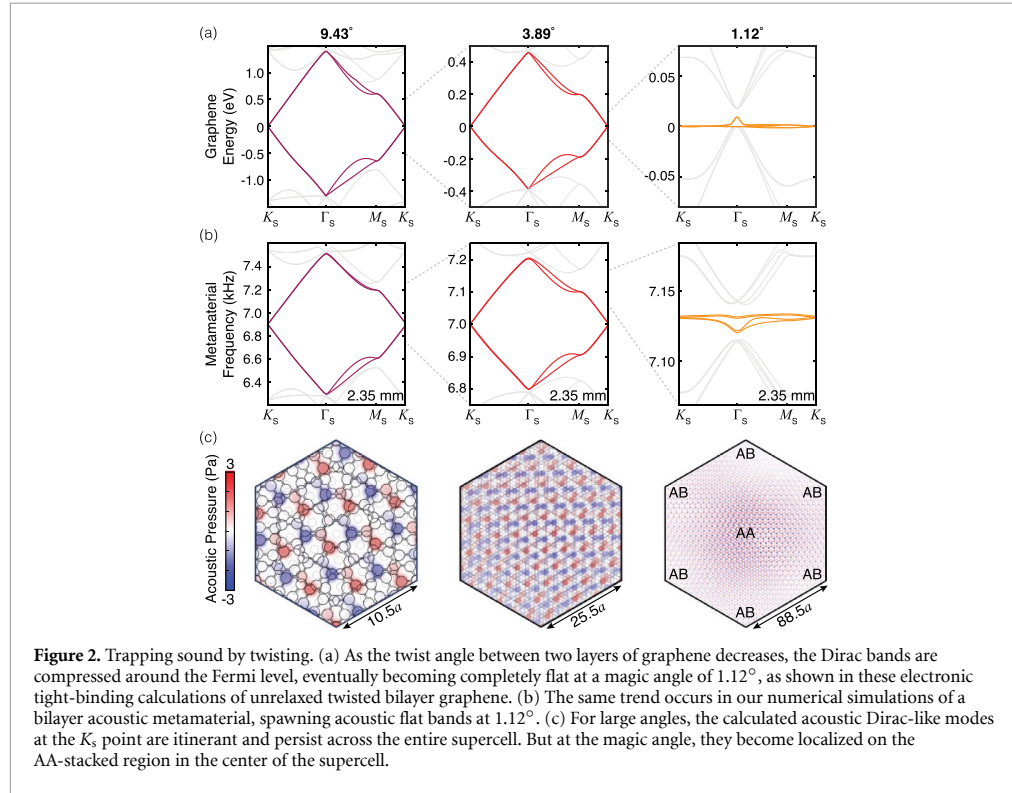
waves [22], and mechanics [23, 24]. Further, it was recently discovered that placing a thin membrane between metamaterial layers can reproduce the coupling effects of vdW forces, yielding acoustic analogs of bilayer and trilayer graphene [25, 26]. The inclusion of a twist angle between metamaterial layers has the potential to further expand their utility. In addition to electronic systems, moiré engineering has recently been demonstrated in systems containing vibrating plates [27], spoof surface-acoustic waves [28], and optical lattices [29]. However, without simultaneous control of in-plane hopping, interlayer coupling, and twist angle, rapidly prototyping next-generation twistronic devices using acoustic metamaterials remains an elusive goal.

Here we propose a simple acoustic metamaterial that precisely recreates the band structure of twisted bilayer graphene, including mode localization at a magic angle of 1.12° . We start with a monolayer acoustic metamaterial that implements a tight-binding model describing the low-energy band structure of graphene. By combining two of these monolayers with an intermediate polyethylene membrane, we numerically simulate both stacking configurations of *untwisted* bilayer graphene using finite-element modeling software, COMSOL Multiphysics. Our simulated acoustic analog of *twisted* bilayer graphene hosts flat bands at the same magic angle of $\sim 1.1^\circ$ as its quantum counterpart [6, 30]. A key advantage of our metamaterial is the ease with which it reaches coupling conditions beyond those feasible

in atomic bilayer graphene. By tuning the thickness of the interlayer membrane, we design new metamaterials that host flat bands at several magic angles between 1.12° and 6.01° . Our results demonstrate the potential for acoustic vdW metamaterials to precisely simulate and explore the ever-growing number of quantum twistronic materials.

2. Results and discussion

We begin by introducing a general framework for designing acoustic metamaterials to prototype non-interacting electronic materials that are well described by a tight-binding model. In our metamaterial, each atomic site is represented by a cylindrical air cavity in a steel plate (see figure 1(a)). The radius of the air cavity determines the eigenfrequencies of its ladder of acoustic standing modes. In a lattice of these cavities, the degenerate standing modes form narrow bands, separated from each other by a large frequency gap. We focus primarily on the lowest, singly degenerate s band. Just as electrons hop from atom to atom in an electronic tight-binding model, sound waves propagate from cavity to cavity in our acoustic metamaterial through a network of tunable thin air channels. This coupling is always positive for s cavity modes, but either sign can be realized by starting with higher-order cavity modes [31]. Because sound travels much more easily through air than through steel, these channels are the dominant means of acoustic transmission through our metamaterial.



They allow nearest- and next-nearest-neighbor coupling to be controlled independently by varying the width or length of separate air channels, providing a platform to implement a broad class of tight-binding models.

To recreate bilayer graphene in an acoustic metamaterial, we started from a honeycomb lattice of air cavities, with radius of 3.5 mm and a separation of 10 mm, in a 1 mm thick steel sheet, encapsulated by 1 mm thick polyethylene boundaries. Each cavity is coupled to its three nearest neighbors using 0.875 mm wide channels, giving an s -mode bandwidth of $2t = 7.8$ kHz (see figure 1(b)). This s manifold is well isolated from other higher-order modes in the lattice, which appear above 25 kHz. The C_6 symmetry of our metamaterial ensures a linear crossing at the K point, similar to the Dirac cone in graphene [32]. The frequency of this Dirac-like crossing and other key aspects of the band structure are controlled by the dimensions of the cavities and channels. Building on previous work, we coupled two layers of acoustic graphene together using a thin interlayer membrane [26]. By laterally translating the stacking configuration, the same acoustic metamaterial mimics both the parabolic touching around the K point seen in AB-stacked bilayer graphene, and the offset Dirac bands seen in AA-stacked bilayer graphene [33, 34], as shown in figures 1(c) and (d).

The frequency span between the K -point eigenmodes is twice the interlayer coupling strength Δ , which is set by the interlayer membrane thickness [26]. We found that a 2.35 mm thick polyethylene membrane (density 950 kg m^{-3} and speed of sound 2460 m s^{-1}) accurately matched the dimensionless coupling ratio $\Delta/t \approx 5\%$ in bilayer graphene.

Introducing a twist angle between two graphene layers creates a moiré pattern that grows in size as the angle decreases. At small angles, the Dirac cones from each layer are pushed together and hybridize due to the interlayer coupling [35, 36], as shown in figure 1(e). Eventually, they form a flat band with a vanishing Fermi velocity (v_F) at a so-called magic angle [6, 30, 37], see figure 2(a). We searched for the same band-flattening mechanism by introducing a commensurate-angle twist to our acoustic bilayer graphene metamaterial. Strikingly, our metamaterial mimics its quantum counterpart even down to the magic angle, producing acoustic flat bands at 1.12° , as shown in figures 2(a) and (b). Importantly, there are no other acoustic bands near the Dirac point that can fold and interfere with these flat bands (see figure 1(b)). The flat bands appear upside down in our acoustic model because its interlayer coupling (between s cavity modes) has the opposite sign from graphene's (between p_z orbitals). However, this asymmetry is quite small and its influence is not generally

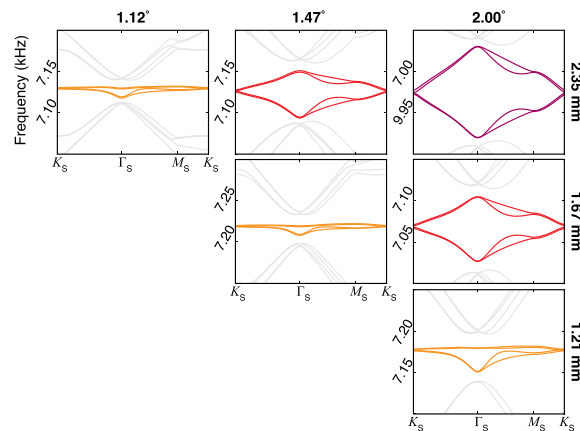


Figure 3. Interlayer coupling tunes the magic angle. Reducing the thickness of the polyethylene membrane enhances the coupling between layers of our simulated acoustic metamaterial. Consequently, an acoustic flat band (orange) can be formed either by decreasing the twist angle with a fixed membrane thickness (along rows), or by decreasing the thickness at fixed angle (columns). For example, to realize flat bands at 2° , we need to reduce the membrane thickness to 1.21 mm.

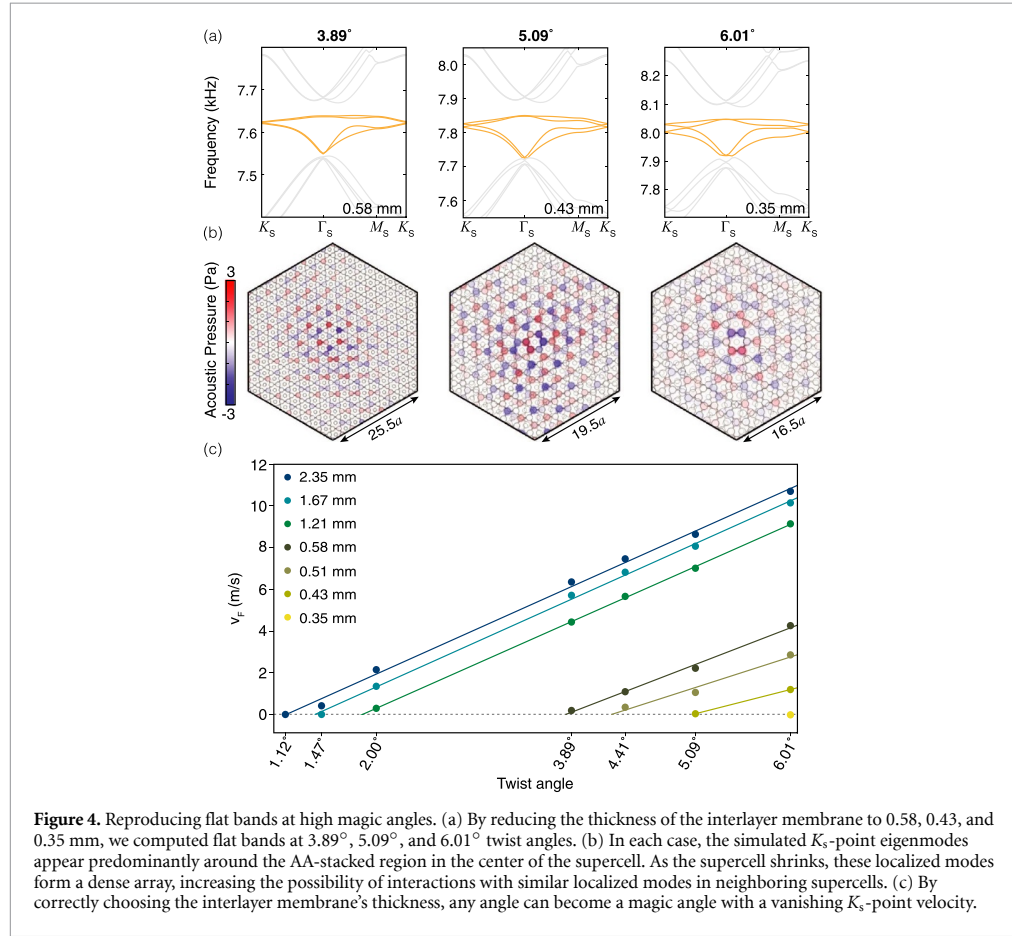
noticeable at higher angles [30, 38]. Our acoustic flat bands correspond to real-space pressure modes that are primarily located on the AA region, see figure 2(c). This AA localization agrees with calculations of the local electronic density of states in magic-angle twisted bilayer graphene [6, 39]. In our acoustic system, these localized modes represent sound waves that propagate with a low group velocity of 0.05 m s^{-1} , compared to 30 m s^{-1} in the untwisted bilayer.

The magic angle of twisted bilayer graphene can be tuned by applying vertical pressure to push the graphene layers closer together and increase the interlayer coupling [40]. Consequently, the Dirac bands begin to flatten at higher angles under pressure than at ambient conditions. However, a substantial vertical pressure of a few GPa is required to move the magic angle from 1.1° to 1.27° , corresponding to only a 20% increase in the interlayer coupling strength [12]. In our metamaterial, no such physical restrictions apply: the interlayer coupling can be tuned over two orders of magnitude simply by changing the thickness of the coupling membrane [26]. In practice, we anticipate an experimental setup that includes interchangeable polyethylene sheets of different thicknesses. To demonstrate this capability, we numerically reproduced the band flattening at a fixed angle of 2° simply by incrementally reducing the thickness of the interlayer membrane to 1.21 mm (figure 3). In other words, the flat band condition can be approached from two directions: either reduce the twist angle at fixed interlayer thickness, or reduce the thickness at fixed angle. For comparison, it is expected to require about 9 GPa of vertical pressure for twisted bilayer graphene to reach flat bands at 2° [40].

Our acoustic metamaterial provides a simple computational platform to explore twistronics in extreme coupling regimes, well beyond the

experimental capability of its electronic counterpart. By further reducing the interlayer membrane thickness, we searched for flat bands at high commensurate angles of 3.89° , 5.09° , and 6.01° , equivalent to pressures of 45, 85, and 129 GPa that would need to be applied to the graphene system [40]. In each case, we discovered flat bands similar to those in twisted bilayer graphene (figure 4(a)). These flat bands all correspond to collective pressure modes that are localized on the AA-stacked central regions (figure 4(b)). But these localized modes are over five times closer to each other spatially at 6.01° than they are at 1.12° . Generally speaking, the modes interact more strongly as they become closer together, potentially allowing interactions to dominate over the reduced kinetic energy at a high magic angle. Consequently, a high-magic-angle metamaterial could be susceptible to non-linear effects if tuned correctly, akin to a phonon-phonon interaction. In principle, any twist angle can become a magic angle that hosts a dense array of such localized modes, by choosing the correct interlayer thickness (figure 4(c)).

Although we focused on recreating twisted bilayer graphene, our metamaterial can be easily extended to capture other vdW systems. For example, by breaking the sublattice symmetry in our unit cell, one can explore the localized modes shaped from twisted quadratic bands, imitating semiconductors like hexagonal boron nitride [41] or transition-metal dichalcogenides [42]. Our metamaterial platform could even mimic twistronic Hamiltonians that cannot yet be realized in condensed matter experiments, which are restricted to the primarily-hexagonal set of 2D materials available today. In principle, a twistronic heterostructure can be constructed from any lattice symmetry to spawn diverse



flat bands with distinct topologies [43]. Acoustic metamaterials can smoothly deform between these twistrionic phases, allowing their properties to be isolated, optimized, or combined. Further, our metamaterial design can independently control AA and AB coupling by appropriately texturing the interlayer membrane, which may unlock perfectly flat bands at the magic angle [44]. It can also implement tunable in-plane lattice relaxation, which modifies both the electronic [45, 46] and phononic [47, 48] bands in twisted bilayer graphene. Beyond two-layer systems, our design motivates a future experimental setup to explore the intricate moiré patterns created by multiple arbitrary twist angles. Such experimental acoustic devices may quickly surpass theoretical electronic calculations, which are made nearly impossible by the highly incommensurate geometry, even in the three-layer case [49]. Importantly, our design translates to the length scales and materials required for photonic [19] or surface-acoustic-wave [22] devices, which may provide a more-natural platform to fabricate the large arrays required to study complex multilayer structures.

3. Conclusion

The enormous phase space of twisted vdW heterostructures promises many new phenomena, but unearthing them is hindered by theoretical and experimental obstacles. Our twisted bilayer metamaterial translates the field of twistrionics to acoustics, opening a different path to continue this search (see roadmap in supplement (available online at stacks.iop.org/2DM/8/031002/mmedia)). By introducing a twist angle to vdW metamaterials, we discovered flat bands that *precisely* mimic the behavior of twisted bilayer graphene at 1.1° and that slow transmitted sound by a factor of 600 (20 times slower than a leisurely walk). The close agreement between our acoustic system and its electronic counterpart gives confidence that twisted acoustic metamaterials can be a valuable platform for more general quantum material design. For example, future 3D-printed acoustic metamaterials could simulate multilayer twistrionic heterostructures containing several independent twist angles, a challenging regime for today's theoretical tools. Meanwhile, recent experiments have demonstrated

control of surface acoustic waves in the quantum limit [50, 51], which could provide a new direction to incorporate phonon-phonon interactions into our acoustic system.

4. Methods

We simulate three-dimensional metamaterial models using the pressure acoustics, frequency domain interface within the acoustics module of COMSOL Multiphysics. A basic monolayer metamaterial consists of a honeycomb arrangement of air cavities, with radius of 3.5 mm and a separation of 10 mm, in a 1 mm thick steel sheet. To form a bilayer metamaterial, two such steel sheets are separated and bounded by three identical polyethylene membranes, as shown in figure 1(a). The bounding and interlayer membranes all have identical, tunable thicknesses. Each model is cut to form a supercell at a commensurate twist angle, allowing three pairs of Floquet periodic boundary conditions on its six hexagonal sides. The top and bottom boundary sheets are impedance-matched to air on their outer faces. Our metamaterial contains three materials: steel plates (density 7070 kg m^{-3} and speed of sound 5790 m s^{-1}), air cavities (1.2 kg m^{-3} , 343 m s^{-1}), and high-density polyethylene interlayer and outer boundary membranes (950 kg m^{-3} , 2460 m s^{-1}). The mesh conditions we use depend on the size of the unit cell. For the monolayer and untwisted bilayer metamaterials, as well as twisted bilayer metamaterials with twist angles above 3.89° , we use the physics-controlled ‘fine’ mesh. For models with lower twist angles, we switch to a coarser user-defined mesh with the following parameters: minimum element size 0.09, maximum element size 1, maximum growth rate 1.45, curvature factor 0.5, and resolution 0.6. After constructing the appropriate metamaterial supercell, we create an eigenfrequency study using the following parametric sweep. For a hexagonal supercell with moiré length L , we simulate the \mathbf{k} -space sweep around the supercell Brillouin zone along the path $\Gamma_s \rightarrow K_s \rightarrow M_s \rightarrow \Gamma_s$ using the following equation:

$$\mathbf{k} = \frac{\pi}{3\sqrt{3}L} \begin{cases} \begin{pmatrix} 4a \\ 0 \end{pmatrix} & 0 < a < 1 \\ \begin{pmatrix} 6-2a \\ \sqrt{3}(2a-1) \end{pmatrix} & 1 < a < 1.5 \\ \begin{pmatrix} 3+3\sqrt{3}-2\sqrt{3}a \\ 3+\sqrt{3}-2a \end{pmatrix} & 1.5 < a < \frac{3+\sqrt{3}}{2}, \end{cases}$$

where a is an arbitrary sweep parameter. To speed up computation, we typically calculate only the 10 eigenfrequencies closest to the Dirac frequency.

The electronic band structures of twisted bilayer graphene displayed in figure 2(a) were generated using a tight-binding model based on density functional theory (DFT) results for bilayer graphene [52].

For the selected angles, we use a twisted commensurate supercell alongside the DFT-derived couplings to populate an electronic k -dependent Hamiltonian, which we then diagonalize. Although atomic relaxations are known to modify the magic angle and the low-energy band gaps between the flat bands and nearby bands in quantum materials [38], we do not attempt to incorporate analogous relaxations in our metamaterial.

Data availability statement

The data that support the findings of this study are available upon reasonable request from the authors.

Acknowledgments

We thank Alex Kruchkov, Haoning Tang, Clayton DeVault, Daniel Larson, Nathan Drucker, Ben November, Walker Gillett, and Fan Du for insightful discussions. The computations in this paper were run on the FASRC Cannon cluster supported by the FAS Division of Science Research Computing Group at Harvard University. This work was supported by the National Science Foundation Grant No. OIA-1921199 and the Science Technology Center for Integrated Quantum Materials Grant No. DMR-1231319. W D acknowledges support from a Herchel Smith Scholarship.

ORCID iDs

S Minhal Gardezi  <https://orcid.org/0000-0002-0012-5546>
 Harris Pirie  <https://orcid.org/0000-0002-5752-5065>
 Stephen Carr  <https://orcid.org/0000-0002-2749-8625>
 William Dorrell  <https://orcid.org/0000-0002-6748-3401>
 Jennifer E Hoffman  <https://orcid.org/0000-0003-2752-5379>

References

- [1] Liang S J, Cheng B, Cui X and Miao F 2020 Van der Waals heterostructures for high-performance device applications: challenges and opportunities *Adv. Mater.* **32** 1903800
- [2] Geim A K and Grigorieva I V 2013 Van der Waals heterostructures *Nature* **499** 419
- [3] Ajayan P, Kim P and Banerjee K 2016 Two-dimensional van der Waals materials *Phys. Today* **69** 38
- [4] Novoselov K S, Mishchenko A, Carvalho A and Castro Neto A H 2016 2D materials and van der Waals heterostructures *Science* **353** aac9439
- [5] Carr S, Massatt D, Fang S, Cazeaux P, Luskin M and Kaxiras E 2017 Twistronics: manipulating the electronic properties of two-dimensional layered structures through their twist angle *Phys. Rev. B* **95** 075420
- [6] Cao Y *et al* 2018 Correlated insulator behaviour at half-filling in magic-angle graphene superlattices *Nature* **556** 80

- [7] Regan E C *et al* 2020 Mott and generalized Wigner crystal states in WSe₂/WS₂ moiré superlattices *Nature* **579** 359
- [8] Jin C *et al* 2019 Observation of moiré excitons in WSe₂/WS₂ heterostructure superlattices *Nature* **567** 76
- [9] Seyler K L, Rivera P, Yu H, Wilson N P, Ray E L, Mandrus D G, Yan J, Yao W and Xu X 2019 Signatures of moiré-trapped valley excitons in MoSe₂/WSe₂ heterobilayers *Nature* **567** 66
- [10] Tran K *et al* 2019 Evidence for moiré excitons in van der Waals heterostructures *Nature* **567** 71
- [11] Cao Y, Fatemi V, Fang S, Watanabe K, Taniguchi T, Kaxiras E and Jarillo-Herrero P 2018 Unconventional superconductivity in magic-angle graphene superlattices *Nature* **556** 43
- [12] Yankowitz M, Chen S, Polshyn H, Zhang Y, Watanabe K, Taniguchi T, Graf D, Young A F and Dean C R 2019 Tuning superconductivity in twisted bilayer graphene *Science* **363** 1059
- [13] Chen G *et al* 2019 Signatures of tunable superconductivity in a trilayer graphene moiré superlattice *Nature* **572** 215
- [14] Ge H, Yang M, Ma C, Lu M H, Chen Y F, Fang N and Sheng P 2018 Breaking the barriers: advances in acoustic functional materials *Natl Sci. Rev.* **5** 159
- [15] Peri V, Serra-Garcia M, Ilan R and Huber S D 2019 Axial-field-induced chiral channels in an acoustic Weyl system *Nat. Phys.* **15** 357
- [16] Serra-Garcia M, Peri V, Süsstrunk R, Bilal O R, Larsen T, Villanueva L G and Huber S D 2018 Observation of a phononic quadrupole topological insulator *Nature* **555** 342
- [17] Ni X, Weiner M, Alù A and Khanikaev A B 2019 Observation of higher-order topological acoustic states protected by generalized chiral symmetry *Nat. Mater.* **18** 113
- [18] Peri V *et al* 2020 Experimental characterization of fragile topology in an acoustic metamaterial *Science* **367** 797
- [19] Mei J, Wu Y, Chan C T and Zhang Z Q 2012 First-principles study of Dirac and Dirac-like cones in phononic and photonic crystals *Phys. Rev. B* **86** 035141
- [20] Torrent D and Sánchez-Dehesa J 2012 Acoustic analogue of graphene: observation of Dirac cones in acoustic surface waves *Phys. Rev. Lett.* **108** 174301
- [21] Lu J, Qiu C, Xu S, Ye Y, Ke M and Liu Z 2014 Dirac cones in two-dimensional artificial crystals for classical waves *Phys. Rev. B* **89** 134302
- [22] Yu S Y *et al* 2016 Surface phononic graphene *Nat. Mater.* **15** 1243
- [23] Torrent D, Mayou D and Sánchez-Dehesa J 2013 Elastic analog of graphene: dirac cones and edge states for flexural waves in thin plates *Phys. Rev. B* **87** 115143
- [24] Kariyado T and Hatsugai Y 2016 Manipulation of dirac cones in mechanical graphene *Sci. Rep.* **5** 18107
- [25] Lu J, Qiu C, Deng W, Huang X, Li F, Zhang F, Chen S and Liu Z 2018 Valley topological phases in bilayer sonic crystals *Phys. Rev. Lett.* **120** 116802
- [26] Dorrell W, Pirie H, Gardezi S M, Drucker N C and Hoffman J E 2020 van der Waals metamaterials *Phys. Rev. B* **101** 121103(R)
- [27] Rosendo López M, Peñaranda F, Christensen J and San-Jose P 2020 Flat bands in magic-angle vibrating plates *Phys. Rev. Lett.* **125** 214301
- [28] Deng Y, Oudich M, Gerard N J, Ji J, Lu M and Jing Y 2020 Magic-angle bilayer phononic graphene *Phys. Rev. B* **102** 180304
- [29] Wang P, Zheng Y, Chen X, Huang C, Kartashov Y V, Torner L, Konotop V V and Ye F 2020 Localization and delocalization of light in photonic moiré lattices *Nature* **577** 42
- [30] Bistrizter R and MacDonald A H 2011 Moiré bands in twisted double-layer graphene *Proc. Natl Acad. Sci. USA* **103** 12233
- [31] Matlack K H, Serra-Garcia M, Palermo A, Huber S D and Daraio C 2018 Designing perturbative metamaterials from discrete models *Nat. Mater.* **17** 323
- [32] Kogan E and Nazarov U V 2012 Symmetry classification of energy bands in graphene *Phys. Rev. B* **85** 115418
- [33] de Andres P L, Ramírez R and Vergés J A 2008 Strong covalent bonding between two graphene layers *Phys. Rev. B* **77** 045403
- [34] McCann E and Koshino M 2013 The electronic properties of bilayer graphene *Rep. Prog. Phys.* **76** 056503
- [35] Shallcross S, Sharma S, Kandelaki E and Pankratov O A 2010 Electronic structure of turbostratic graphene *Phys. Rev. B* **81** 165105
- [36] Moon P and Koshino M 2013 Optical absorption in twisted bilayer graphene *Phys. Rev. B* **87** 205404
- [37] Suárez Morell E, Correa J D, Vargas P, Pacheco M and Barticevic Z 2010 Flat bands in slightly twisted bilayer graphene: tight-binding calculations *Phys. Rev. B* **82** 121407(R)
- [38] Carr S, Fang S, Zhu Z and Kaxiras E 2019 Exact continuum model for low-energy electronic states of twisted bilayer graphene *Phys. Rev. Res.* **1** 013001
- [39] Kim K *et al* 2017 Tunable moiré bands and strong correlations in small-twist-angle bilayer graphene *Proc. Natl Acad. Sci. USA* **114** 3364
- [40] Carr S, Fang S, Jarillo-Herrero P and Kaxiras E 2018 Pressure dependence of the magic twist angle in graphene superlattices *Phys. Rev. B* **98** 085144
- [41] Xian L, Kennes D M, Tancogne-Dejean N, Altarelli M and Rubio A 2019 Multiband bands and strong correlations in twisted bilayer boron nitride: doping-induced correlated insulator and superconductor *Nano Lett.* **19** 4934
- [42] Naik M H and Jain M 2018 Ultraflatbands and shear solitons in moiré patterns of twisted bilayer transition metal dichalcogenides *Phys. Rev. Lett.* **121** 266401
- [43] Kariyado T and Vishwanath A 2019 Flat band in twisted bilayer bravais lattices *Phys. Rev. Res.* **1** 033076
- [44] Tarnopolsky G, Kruchkov A J and Vishwanath A 2019 Origin of magic angles in twisted bilayer graphene *Phys. Rev. Lett.* **122** 106405
- [45] Angeli M, Mandelli D, Valli A, Amaricci A, Capone M, Tosatti E and Fabrizio M 2018 Emergent D₆ symmetry in fully relaxed magic-angle twisted bilayer graphene *Phys. Rev. B* **98** 235137
- [46] Yoo H *et al* 2019 Atomic and electronic reconstruction at the van der Waals interface in twisted bilayer graphene *Nat. Mater.* **18** 448
- [47] Koshino M and Son Y W 2019 Moiré phonons in twisted bilayer graphene *Phys. Rev. B* **100** 075416
- [48] Lamparski M, Van Troeye B and Meunier V 2020 Soliton signature in the phonon spectrum of twisted bilayer graphene *2D Mater.* **7** 025050
- [49] Zhu Z, Carr S, Massatt D, Luskin M and Kaxiras E 2020 Twisted trilayer graphene: a precisely tunable platform for correlated electrons *Phys. Rev. Lett.* **125** 116404
- [50] Satzinger K J *et al* 2018 Quantum control of surface acoustic-wave phonons *Nature* **563** 661
- [51] Chu Y, Kharel P, Yoon T, Frunzio L, Rakich P T and Schoelkopf R J 2018 Creation and control of multi-phonon Fock states in a bulk acoustic-wave resonator *Nature* **563** 666
- [52] Fang S and Kaxiras E 2016 Electronic structure theory of weakly interacting bilayers *Phys. Rev. B* **93** 235153